

1 ***Cladosporium herbarum* peptidogalactomannan**
2 **triggers significant defense responses in whole tobacco**
3 **plants**

4 **Caroline de B. Montebianco^{1,2}, Bianca B. Mattos^{2,3}, Tatiane da F Silva⁴, Eliana**
5 **Barreto-Bergter², Maite F S Vaslin¹**

6 ¹Departamento de Virologia, Instituto de Microbiologia Paulo de Góes (IMPPG), UFRJ, Rio de
7 Janeiro, RJ, Brazil

8

9 ²Departamento de Microbiologia Geral, Instituto de Microbiologia Paulo de Góes (IMPPG),
10 UFRJ, Rio de Janeiro, RJ, Brazil.

11

12 ³Embrapa Solos, Jardim Botânico. RJ, Brazil

13

14 ⁴Escola de Engenharia de Lorena (EEL), Departamento de Biotecnologia (Debiq), Universidade
15 de São Paulo (USP)

16

17 **Abstract**

18

19 *Cladosporium herbarum* is one of the most frequently occurring fungal species, with a
20 worldwide distribution, and is found in almost all man-occupied niches in organic and
21 inorganic matter and as a phytopathogen on certain agricultural crops. The structure of
22 the most abundant glycoprotein from the *C. herbarum* cell wall, peptidogalactomannan
23 or pGM, was previously elucidated and includes carbohydrates (76%), with mannose,
24 galactose and glucose as its main monosaccharides (52:36:12 molar ratio). pGM was
25 able to strongly induce the expression of defense-related genes and ROS accumulation
26 when in contact with BY2 tobacco cells. Here, using two distinct *Nicotiana tabacum*
27 cultivars, Xanthi and SR1, we evaluated the ability of *C. herbarum* pGM to induce
28 SAR-like defense by studying its antiviral activity against *Tobacco mosaic virus* (TMV)
29 and the induction of SAR markers including *PR* genes and ROS accumulation. Our
30 results show that pGM induced a strong activation of defense responses in treated plants
31 from both tobacco cultivars, contributing to the impairment of viral infection.
32 Expression levels of the pathogenesis-related genes *PR-1a* (unknown function), *PR-2*
33 (β -1-3 *endoglucanase*), *PR-3* (*chitinase*), and *PR-5* (*thaumatin-like protein*), the
34 phenylpropanoid pathway gene *PAL* (*phenylalanine ammonia-lyase*) and genes
35 involved in plant stress responses and innate immunity, such as *LOX1* (*lipoxygenase*)

36 and *NtPrxNI* (*peroxidase*), were strongly induced until 120 h after pGM spray
37 application. Accumulation of superoxide radicals was also observed in a pGM dose-
38 dependent manner.

39

40 **Introduction**

41 To face pathogen attack, plants have developed important pathways of
42 response against infections, which include mainly the immunity associated with the
43 recognition of conserved pathogen or microbe molecular patterns (PAMPs/MAMPs),
44 such as fungal chitin or bacterial flagellin by plant cell receptors (PRRs) (reviewed by
45 e.g. [1]). This first line of response is called PAMP-triggered immunity (PTI). To
46 overcome PTI, pathogens develop effector molecules that enable them to successfully
47 infect a host even when PTI is active. Plants, however, can face this by a second line of
48 defense, effector-triggered immunity (ETI) [2, 3]. PTI may result in a decrease in
49 pathogen colonization, consequently blocking the disease development and conferring
50 basal resistance. Second, ETI confers resistance later, often resulting in a hypersensitive
51 response (HR). Immunity directly associated with pathogen effectors is triggered by
52 host cell identification of the effector itself or by effector-induced responses. This
53 recognition accelerates and amplifies PTI-mediated responses, often leading to an HR at
54 infection sites and to a systemic induction of resistance known as systemic acquired
55 resistance (SAR). Once properly stimulated, SAR provides long-term defense against a
56 broad spectrum of pathogens [4-8]. Therefore, a localized microbial infection in a single
57 or in some leaves can immunize the rest of the plant against a subsequent infection. This
58 phenomenon makes the plant temporally resistant to new infection events even if the
59 subsequent infection occurs at a site far from the initial primary site.

60 *Cladosporium herbarum* is a fungus that is not pathogenic to humans, but the easy
61 dispersion of its spores in air makes it an important airway allergen, leading to the
62 development of respiratory diseases such as rhinitis, conjunctivitis and asthma [9]. In
63 addition, it has also been described as a phytopathogen in some agricultural crops, such
64 as passion fruit and corn. *C. herbarum* infects passion fruit, causing cladosporiosis,
65 which reduces fruit production and quality [10]. In corn, it causes *Cladosporium* ear rot
66 [11]. Cladosporiosis can occur by contaminated seedlings or wind-dispersed conidia
67 [12], potentially affecting any aerial parts of the plant but mainly growing tissues such

68 as leaves, branches, flower buds and fruits, negatively impacting plant development and
69 production [13].

70 The cell walls of members of the *Cladosporium* genus have a complex composition
71 consisting mainly of polysaccharides (80-90%) and, to a lesser extent, proteins,
72 glycoproteins and lipids [14]. Chitin and β -glucans are the main polysaccharides and are
73 located in the inner layer of the cell wall, whereas glycoproteins are anchored in the
74 outermost layer [15-17]. Fungal cell wall composition may vary according to the
75 morphological type, growth stage and fungal species and is different from the plant cell
76 wall composition, which mainly includes cellulose [18]. Among the fungal cell wall
77 glycoproteins, peptidogalactomannan (pGM) can be found in various fungi, such as
78 *Cladosporium werneckii*, *C. resinae*, *Aspergillus fumigatus*, *Aspergillus wentii*,
79 *Malassezia* species and *Chaetosartorya chrysella* [19-22].

80 In a previous study, the *Cladosporium herbarum* pGM structure was elucidated and
81 found to include carbohydrates (76%) and mannose, galactose and glucose as its main
82 monosaccharides (52:36:12 molar ratio). The presence of a main chain containing
83 (1 \rightarrow 6)-linked α -D-Man_p residues was observed by methylation and ¹³C-nuclear
84 magnetic resonance (¹³C-NMR) spectroscopy [23]. β -D-Galactofuranosyl residues were
85 present as (1 \rightarrow 5)-interlinked side chains of *C. herbarum* pGM. The role of pGM cell
86 wall glycoprotein in plant-fungus interactions was first studied by Mattos *et al.* [23],
87 who showed the induction of the expression of defense genes in tobacco BY2 cells and
88 a hypersensitive response (HR) after treatment of tobacco leaves with *C. herbarum*
89 pGM. This recognition and defense response activation would possibly contribute to the
90 plant response to the pathogen attack, protecting itself against new infections and
91 indicating that pGM is probably able to induce SAR.

92 Here, using two distinct *Nicotiana tabacum* cultivars, Xanthi and SR1, we evaluated the
93 ability of *C. herbarum* pGM to induce antiviral activity against *Tobacco mosaic virus*
94 (TMV), PR genes and oxygen-reactive species (ROS) accumulation. Our results showed
95 that pGM treatment induced a SAR-like response in both tobacco cultivars with strong
96 activation of defense responses by the treated plants, enabling them to impair the viral
97 infection.

98

99 **Material and Methods**

100 **Strain and culture conditions**

101 *Cladosporium herbarum*, CBS 121621, was provided by Dr J. Guarro,
102 Advanced Studies Institut, Réus, Spain and was maintained in potato dextrose broth
103 (PDB/Acumedica) in Erlenmeyer flasks at room temperature for 7 days with shaking.
104 Mycelium was obtained via filtration, washed with distilled water and stored at -20°C.

105

106 **Extraction of *C. herbarum* glycoprotein**

107 Crude glycoprotein extraction was performed according to [22]. Briefly, *C.*
108 *herbarum* mycelium was extracted with 0.05 M phosphate buffer, pH 7.2, at 100°C for
109 2 h. The mixture was filtered, and the filtrate was evaporated into a small volume and
110 precipitated with three volumes of ethanol overnight at 4°C. The precipitate was
111 dialyzed and freeze-dried to obtain the crude glycoprotein (pGM). pGM purity was
112 checked by HPTLC and GC-MS as described by Mattos *et al.*, [23] and no
113 contaminants were present.

114

115 **Plant growth and pGM treatment**

116 *N. tabacum* cv. Xanthi and cv. SR1 seeds were germinated and grown in
117 substrate in a greenhouse at $25 \pm 2^\circ\text{C}$ with a natural photoperiod. Young adult tobacco
118 plants with 4-6 true leaves were sprayed with $600 \mu\text{g}\cdot\text{ml}^{-1}$ of water diluted pGM with a
119 high-pressure apparatus (W550, Wagner) according to [24]. MilliQ water was sprayed
120 as control. Four pGM assay experiments were performed with Xanthi cv. with 16 plants
121 sprayed with pGM and mechanically infected with TMV 24 h later and 16 plants
122 sprayed with water and mechanically infected with TMV 24 h later in each experiment.
123 Plants without treatment were used as healthy controls, plants only mechanically
124 inoculated with TMV were used as TMV inoculation controls, plants treated with pGM
125 were used as pGM control plants, and plants just sprayed with water were used as water
126 treated (H_2O) controls (mock). pGM assays with SR1 cv. were carried out 3 times with
127 10 plants used for each control (healthy plants, pGM alone, H_2O -mock and TMV alone)
128 and 15 plants for pGM + TMV and 15 for H_2O + TMV in each experiment.
129 Immediately before spraying, pGM was resuspended in MilliQ water, and the
130 suspension was sterilized by filtration in a Millipore $0.20 \mu\text{m}$ filter.

131

132 ***Tobacco mosaic virus (TMV) infection and evaluation of*** 133 **disease severity**

134 For TMV mechanical infection, 1 g of TMV-infected frozen leaves (-80° C) was
135 ground with a mortar and pestle in 19 ml of 0.01 M potassium phosphate buffer pH 7.0
136 to obtain the viral suspension [25]. Twenty-four hours after water or pGM treatment, the
137 first 3 true leaves of each plant were mechanically inoculated with TMV without the use
138 of abrasive. Experiments were carried out 4x with *N. tabacum* Xanthi and 3x with *N.*
139 *tabacum* SR1 plants.

140 For cv. Xanthi, 48 hours post infection (hpi) with TMV, the disease incidence was
141 measured by direct counting of necrotic lesions in each infected leaf, as described by
142 [26], where the number of necrotic lesions was expressed as the infection percentage.

143 To assess TMV disease severity in pGM treated cv. SR1 plants, the plants were
144 evaluated by visual observation 25 days post TMV infection (dpi) using a 0-5 disease
145 scale. In this scale, the value 0 corresponds to the absence of symptoms; 1 to one or two
146 leaves showing light mottling; 2 to more than two leaves showing light mottling with
147 few thin yellow veins; 3 to mottling and vein clearing unevenly distributed on the leaf; 4
148 to mottling, leaf distortion, and stunting; and 5 to severe mottling, leaf curling, and
149 stunting. The severity of the disease was quantified using the disease index (DI%)
150 proposed by [27], applying the following formula: $DI = \sum(DS \times P)/(TNP \times HGS) \times 100$,
151 where DS = degree of the scale determined for each plant; P = number of plants
152 showing each degree of infection (score); TNP = total number of plants evaluated; and
153 HGS = highest grade of the scale (maximum infection score).

154

155 **ELISA assays**

156 Enzyme-Linked Immunosorbent Assays (ELISA) analyses were carried out to
157 measure the amount of the virus in leaf samples using PathoScreen® (Agdia) ELISA kit
158 for specific detection of tobamovirus family including TMV following Agdia protocol.
159 Leaf samples of water- and pGM-treated SR1 plants inoculated with TMV were
160 collected 72 h after virus infection. Each sample was ground in a 1:10 (leaf:extraction
161 buffer (Adgia Co.) dilution and then loaded onto ELISA 96-well plates. Tests were
162 performed in technical triplicates and the plates were read using a microplate
163 spectrophotometer from BioRad Co.. Virus quantification was obtained using the
164 standard curve of a 1.0×10^7 TMV particles/g of leaf sample serial dilution.

165

166 **Measurement of superoxide radical accumulation in leaves** 167 **treated with pGM**

168 Evaluation of superoxide radical accumulation was performed using nitroblue
169 tetrazolium (NBT) staining according to [28]. Leaves sprayed with 100, 200, 400 and
170 600 $\mu\text{g}\cdot\text{ml}^{-1}$ of pGM were collected after 24 and 72 h and 8 and 10 days after spray
171 application and incubated with NBT at 0.5 $\text{mg}\cdot\text{ml}^{-1}$ for 1 h in vacuum. Subsequently,
172 leaves were immersed in 95% boiling ethanol until for total removal of chlorophyll.

173

174 **Analysis of defense gene expression by qRT-PCR**

175 Total RNA was extracted from young leaves between 24 and 120 h after
176 treatment with water or 600 $\mu\text{g}\cdot\text{ml}^{-1}$ pGM using TRIzol® Reagent (AmbionRNA by
177 Life Technologies™) according to the manufacturer's instructions. RNA concentration
178 and purity were determined using a NanoDrop2000 Spectrophotometer (Thermo
179 Scientific Co.). RNA integrity was assessed using 1% agarose gel electrophoresis and
180 ethidium bromide staining. One microgram of total RNA from each sample was treated
181 with RQ1 RNase-Free DNase (Promega Co.) according to the manufacturer's
182 instructions. Complementary DNA (cDNA) synthesis was performed with a Revert Aid
183 First Strand cDNA Synthesis Kit (Fermentas Co.) and 100 μM of OligodT primer using
184 1 μg of total RNA as a template, according to the manufacturer's instructions. Following
185 cDNA synthesis, the samples were diluted 25-fold in sterile water. Primers for qPCR,
186 described by [23], were designed for seven defense-related genes (*PR-1a*, *PR-2*, *PR-3*,
187 *PR-5*, *NtPrxNI*, *LOXI* and *NtPAL*) and two constitutively expressed genes (*PP2A* and
188 *Nt-ACT9*). Amplification reactions were performed on an Applied Biosystems® 7500
189 Fast Real-Time PCR apparatus using a 96-well plate. All reactions were performed
190 using two independent biological pools composed of leaves of 5 independent plants
191 each. Three technical triplicates were analyzed for each biological replication. Three
192 negative controls without cDNA were included on the plate for each primer. A mix was
193 performed according to the manufacturer's instructions containing the specific primer
194 pairs for each gene at 10 μM and SYBR Green/ROX qPCR Master Mix (Thermo
195 Scientific). cDNA amplification reactions were performed in a final volume of 25 μl ,
196 according to the manufacturer's guidelines. qPCR cycles were 10 minutes at 95°C for
197 initial denaturation, followed by 40 cycles of denaturation at 95°C for 15 sec and

198 annealing/extension at 60°C for 1 minute, except for the PAL and PR5 genes, for which
199 the annealing temperature was adjusted to 62°C [23]. The results were analyzed by the
200 $2^{-\Delta\Delta CT}$ method according to [29].

201

202 **Statistical analysis**

203 Statistical analyses were performed using GraphPad Prism software version 5.00
204 for Windows using “ONE-WAY ANOVA” Bonferroni test to evaluate if total number
205 of TMV-induced necrotic lesions differ significantly between pGM treated and water-
206 treated plants and compare ELISA results between treatments. Disease severity index
207 between treatments were compared using One Way ANOVA Kruskal-Wallis and
208 Dunn’s Multiple Comparison Test and “TWO-WAY ANOVA” Bonferroni test was
209 used to evaluate qRT-PCR results.

210

211 **Results**

212 **pGM induces tolerance against TMV infection in tobacco**

213 **plants**

214 To evaluate the potential of *C. herbarum* pGM in inducing virus defense in *N.*
215 *tabacum*, tobacco plants from two distinct cultivars were sprayed with 600 µg.ml⁻¹
216 pGM and mechanically inoculated with TMV 24 hours later. Forty-eight hours after
217 TMV infection, plants from the tobacco cultivar Xanthi sprayed with water showed
218 TMV-induced typical necrotic lesions (Fig 1A middle panel). Plants sprayed with pGM,
219 however, showed a reduction in the number of necrotic lesions after TMV infection. A
220 reduction of 42% in the number of necrotic lesions was observed when comparing
221 water- and pGM-treated plants after TMV challenge and of 51% comparing pGM-
222 treated and untreated TMV-infected plants (TMV infection control) (Fig 1B). Statistical
223 analyses, however, showed that the number of necrotic lesions of water-treated and
224 untreated plants were similar. Seven days after TMV infection, leaves at position 3 of
225 plants previously sprayed with water showed 2.6x more necrotic lesions than leaves at
226 the same position of pGM-sprayed plants (Fig 1C and 1D).

227

228 **Figure 1: pGM treatment induced a reduction in the number of TMV induced**
229 **necrotic lesions in *Nicotiana tabacum* cv. Xanthi.** *N. tabacum* cv. Xanthi were treated
230 with water or pGM and mechanically inoculated with TMV 24 hours later. (A) Details
231 of representative leaves 7 dpi with TMV. Upper panel shows TMV infected untreated
232 plants. Middle and bottom panels show leaves from water and pGM-treated plants,
233 respectively. (B) Number of necrotic lesions in pGM treated plants. Dot plots represent
234 the sum of the necrotic lesions observed in leaves 1-3 of each plant after TMV infection
235 in untreated (n=10), H₂O (n=20) and pGM (n=20) treated plants. Horizontal bars
236 represent average values and vertical bars SE. The percentage of necrotic lesions
237 reduction is shown over the dots and *** indicates significant differences with $p <$
238 0.001. (C) pGM treatment experimental scheme. After pulverization, leaves 1-3 were
239 infected with TMV. (D) Total number of TMV-induced necrotic lesions at leaves 1-3
240 after each treatment from a representative experiment. Different letters represent
241 statistical differences between the treatments for each leaf position with a p value $<$
242 0.05. Experiments were repeated two times. pGM - peptidogalactomannan. TMV -
243 *Tobacco mosaic virus*. Bar: 1 cm

244

245 Tobacco plants from the TMV-susceptible cv. SR1 were similarly assayed. Symptoms
246 of TMV infection were evaluated 3 weeks after infection. Typical symptoms of tobacco
247 mosaic disease were visible since 18 dpi on untreated control as well as on water-treated
248 plants. A strong reduction in disease symptoms was observed in pGM-treated plants,
249 where only mild symptoms were observed. Fig 2A shows representative leaves of pGM
250 treated infected plants. A disease severity index was used to compare TMV disease
251 severity of individual plants after each treatment. As shown in Table 1, the pGM
252 treatment induced a decrease between 76-80% in the disease severity compared to
253 treatment with water, suggesting that pre-treatment with pGM could confer protection
254 to the plants against TMV infection. Elisa assays performed in the infected plants
255 showed that viral accumulation decreased 10 times on pGM-treated TMV infected SR1
256 plants compared to water-treated TMV infected plants (Table 1 and Fig 2B).

257 So, pGM treatment was able to induce virus tolerance in both tobacco cvs., with a
258 reduction in the number of necrotic lesions in Xanthi and an important decrease of
259 mosaic disease in SR1.

260

261 **Figure 2: pGM treatment induced TMV tolerance in *N. tabacum* cv. SR1.** *N.*
262 *tabacum* cv. SR1 were treated with water or pGM and mechanically inoculated with
263 TMV after 24 h. (A) Leaves of controls (upper panel) and water and pGM-treated TMV
264 infected plants 22 dpi. (B) TMV accumulation seventy two hours post TMV
265 inoculation. Levels of TMV particles were assayed in water and pGM treated plants by
266 ELISA assay. ODs observed in water and pGM treated plants were plotted in a TMV
267 quantification standard curve. Boxes are showing the average number of TMV particles
268 per g of leaf. Vertical bars are showing SE and the horizontal bar shows ANOVA
269 Bonferroni test comparing viral accumulation on water and pGM treatment with $p <$
270 0.01.

271

272 **Table 1: Response of tobacco SR1 pGM treated plants to tobacco mosaic virus**
273 **(TMV).**

Treatments	Number of symptomatic plants* Experiment 1	Disease severity index (%)** Experiment 1	Number of symptomatic plants* Experiment 2	Disease severity index (%)** Experiment 2	TMV detection by ELISA (415 nm) [§]	TMV quantification
untreated	10/10 a	100.0 a	10/10 a	100.0 a	1.70 ± 0.14 a	1.0 x 10 ⁵ a
H ₂ O	20/20 a	100.0 a	20/20 a	100.0 a	1.29 ± 0.03 a	2.0 x 10 ⁵ a
pGM	12/20 b	20.0 b	14/20 b	24.0 b	0.35 ± 0.17b	1.0 x 10 ⁴ b

274 Number of TMV symptomatic per infected plants (*) and a disease severity index (**)
275 shown by *N. tabacum* cv. SR1 25 dpi with TMV for the distinct treatments from two
276 independent experiments.

277 § - ODs average and SE obtained by TMV ELISA detection at 415 nm.

278 Column 7 shows the average number of TMV particles per g of infected leaf in each
279 treatment.

280 Different letters correspond to significant differences with $p < 0.001$. Statistical analysis
281 was performed using One way ANOVA Bonferroni test (columns 2-4 and 6-7) and
282 Kruskal-Wallis and Dunn's Multiple Comparison Test (columns 3 and 5).

283

284 **ROS accumulation in pGM-treated tobacco plants**

285 It is proposed that ROS can act as defense compounds against viruses [30, 31].
286 H₂O₂ can act as a systemic antiviral signaling molecule during TMV infection;
287 however, the role of ROS in plant-virus interactions is not completely understood [32].
288 The accumulation of ROS is also considered a biochemical marker of SAR induction
289 [31].

290 To check if pGM treatment induces ROS accumulation in the tobacco treated plants, we
291 examined the presence of ROS in the pGM-sprayed plants. Leaves from plants sprayed
292 with different pGM concentrations (100, 200, 400 and 600 $\mu\text{g}\cdot\text{ml}^{-1}$) were analyzed over
293 time, and the presence of superoxide radicals was assayed using nitroblue tetrazolium
294 (NBT) reduction and histological staining. Figure 3 illustrates the accumulation of
295 superoxide radicals after treatment with different pGM concentrations. We observed a
296 dose-dependent effect of pGM spray on superoxide radical accumulation. Superoxide
297 accumulation was observed from 24 h to 10 days after pGM spray for all pGM
298 concentrations analyzed. After 8 days, however, a decay in its accumulation was
299 observed. Curiously, 400 $\mu\text{g}\cdot\text{ml}^{-1}$ pGM showed a stronger induction of superoxide
300 radical accumulation than 600 $\mu\text{g}\cdot\text{ml}^{-1}$, showing that the capacity of ROS induction of
301 pGM may be saturated at higher concentrations. Histological assays to detect the
302 presence of hydrogen peroxide in these plants using 3,3-diaminobenzidine (DAB) were
303 also performed; however, DAB deposition was not observed (data not shown).

304

305 **Figure 3: pGM is inducing superoxide radical accumulation in pGM-treated**
306 **Xanthi plants.** The accumulation of superoxide radicals after spray of pGM at different
307 concentrations (100, 200, 400 and 600 $\mu\text{g}\cdot\text{ml}^{-1}$) was evaluated along 10 days using
308 nitroblue tetrazolium (NBT). Representative leaves of each treatment are shown. dap -
309 days after pGM pulverization. Bar: 1cm.

310

311 **pGM treatment induces defense gene expression in tobacco** 312 **plants**

313 To analyze whether pGM spray induces defense-related gene expression in
314 treated plants, the transcript levels of the *pathogen-related 1-3* and *5* (*PR1 α* , *PR2*, *PR3*
315 and *PR5*), as well as *peroxidase N1* (*NtPrxN1*), *phenylalanine ammonia-lyase* (*PAL*) and
316 *lyxogenase 1* (*LOX1*) genes, were evaluated over time in *N. tabacum* plants from cvs.
317 Xanthi and SR1 after spray application of 600 $\mu\text{g}\cdot\text{ml}^{-1}$ pGM.

318 pGM induced the expression of all PR genes analyzed 24 h after treatment in both
319 tobacco cvs (Fig 4). A very strong induction of the *PR1- α* expression, a classical SAR
320 marker, was observed in Xanthi. Twenty-four hours after pGM spray, *PR1- α* expression
321 was more than 2000-fold compared to that in control plants sprayed with water.
322 However, this gene expression decreased 24 h later and increased again 72 h after pGM

323 treatment but at lower levels than during the first 24 h. Looking at the *PR1- α* expression
324 in cv. SR1, we observed a more pronounced expression at 72 h, reaching approximately
325 300-fold that of the control. An up- and down-regulation cycle was observed in plants
326 from this cv., where we observed an increase of more than 30x in *PR1- α* expression in
327 the first 24 h, followed by a small decrease of 4x at 48 h and again a drastic increase at
328 72 h. After that, *PR1- α* expression levels decreased again at 96 h and returned to high
329 levels at 120 h. In summary, *PR1- α* was strongly induced by pGM treatment in both
330 tobacco cultivars, however, in Xanthi, the induction and its decay occurred earlier than
331 in SR1. The presence of high levels of *PR1* transcripts in SR1 pGM-treated plants after
332 96 and 120 h after pGM spray may indicate that pGM treatment is in fact inducing
333 systemic spreading signals over the sprayed leaves as the leaves samples of these two
334 points developed after pGM treatment.

335

336 **Figure 4: qRT-PCR analysis of some PR genes in water and pGM-treated plants**
337 **between 24 and 120 h after treatment.** Axis y is showing the fold change of *PR1- α* ,
338 *PR2*, *PR3* and *PR5* transcripts levels in *N. tabacum* cv. Xanthi and cv. SR1 after pGM
339 treatment in comparison with water treatment calculated using $2^{-\Delta\Delta C_t}$ method described
340 by [29]. *PP2A* and *NtACT-9* were used as reference genes. The standard deviations are
341 indicated by error bars, and significant differences between fold changes with $p < 0.05$
342 and $p < 0.001$ are indicated by * and ***, respectively. *PR1- α* : Unknown function,
343 possible antifungal function; *PR2*: β - (1,3) endonuclease; *PR3*: chitinase; *PR5*:
344 *thaumatin-like protein*. *PP2A* and *NtACT-9* were used as reference genes.

345

346 Xanthi and SR1 showed 30- and 14-fold increases in *PR-2* (β -1,3 glucanase) gene
347 expression after 24 h, respectively (Fig 4). After this time, however, *PR-2* mRNA levels
348 were little reduced in water- and pGM-treated Xanthi plants and little induced in SR1,
349 showing an early induction only of this specific gene. *PR-3*, which encodes the
350 *chitinase* gene, showed a very low induction (3x) in Xanthi in the first 24 h but an
351 increase of 50x in SR1 plants at the same time. With increasing time, an elevation in its
352 expression was observed, reaching more than 45-fold that of the control at 72 h in
353 Xanthi. SR1 *PR-3* induction mediated by pGM was stronger and peaked at 96 h after
354 pGM treatment (more than 900-fold change expression) and decreased with time.
355 Expression of *PR-5*, which encodes a *thaumatin-like protein* gene, was 45- and 5-times

356 higher than that of the control after 24 h in Xanthi and SR1 plants, respectively,
357 decreasing with time in Xanthi.

358 *NtPrxNI* (*peroxidase*) transcripts were highly induced in Xanthi as well in SR1,
359 reaching values more than 200x at 24 and 72 h and 110x at 72 h in Xanthi and SR1,
360 respectively (Fig 5). The high expression of the *peroxidase* gene may indicate that
361 abnormal levels of ROS accumulated after pGM treatment in both cultivars. Leaves that
362 developed after pGM spray, however, did not show *NtPrxNI* mRNAs induction (Fig 5,
363 96 and 120 h).

364

365 **Figure 5: qRT-PCR analysis of defense related genes in water and pGM-treated**
366 **plants between 24 and 120 hours after treatment.** Axis y is showing average fold
367 changes between transcripts levels of *NtPrxNI* (*peroxidase*), *PAL* (*phenylalanine*
368 *ammonia-lyase*) and *LOX* (*lipoxygenase*) of *N. tabacum* cv. Xanthi and cv. SR1 after
369 pGM treatment in comparison with water treatment calculated using $2^{-\Delta\Delta Ct}$ method
370 described by [29]. *PP2A* and *NtACT-9* were used as reference genes. The standard
371 deviations are indicated by error bars, and significant differences between fold changes
372 with $p < 0.05$ and $p < 0.001$ are indicated by * and ***, respectively.

373

374 The *PAL* (*phenylalanine ammonia-lyase*) gene was also induced in both tobacco
375 cultivars; however, the time course of *PAL* expression was different between them. In
376 Xanthi, expression was induced earlier, reaching its highest level at 24 h after pGM
377 spray application (24x). After this time point, the expression decreased to levels similar
378 to those of the control. In SR1, however, the expression was only 5x more than that of
379 the control at 24 h, reaching a maximum at 120 h, where it was expressed 130-fold
380 compared with the control. *LOX* (*lipoxygenase*) gene, also associated with oxidative
381 stress, was strongly induced (425x) in Xanthi plants at 72 h after pGM treatment. In
382 SR1 plants, a comparatively slighter expression (27x) of this gene was observed,
383 peaking at 24 h after pGM treatment.

384 Our RT-qPCR assays showed that almost all of the *PRs* and defense-related genes
385 analyzed were strongly induced by pGM treatment. Our results indicated that pGM is
386 responsible for the activation of a local systemic defense, observed in samples collected
387 between 24-72 h. Results obtained from SR1 leaves that do not receive pGM directly
388 (collected at 96 and 120 h), suggest that pGM may be an SAR inducer.

389

390 Discussion

391 The present work aims to unravel the role of the *C. herbarum* cell wall
392 peptidogalactomannan (pGM) as a plant defense elicitor. Treatment of young *Nicotiana*
393 *tabacum* cv. Xanthi plants with pGM before TMV infection caused a reduction of 51
394 and 42% in the number of TMV-induced necrotic lesions when compared with
395 untreated plants and water-sprayed plants, respectively. In *N. tabacum* cv. SR1 plants,
396 decrease of 76-80% in disease severity was detected after treatment with *C. herbarum*
397 pGM, showing that pGM treatment is able to promote protection against the viral
398 pathogen in both tobacco cvs. In agreement, ELISA assays confirmed a reduction in the
399 viral accumulation after treatment. In addition, we also observed a dose-dependent
400 accumulation of superoxide radicals in pGM-treated plants. Superoxide radical
401 accumulation seemed to be especially high during the first 24 h after pGM treatment,
402 decreasing after 10 days. It was interesting to observe that even doses lower than 600
403 $\mu\text{g}\cdot\text{ml}^{-1}$, used in this work, and 400 $\mu\text{g}\cdot\text{ml}^{-1}$, previously used with BY2 tobacco cells
404 [23], were able to induce the accumulation of superoxide radicals, indicating that
405 oxidative stress mediated by ROS is induced in leaves after pGM treatment. A
406 significant strong increase in expression of *NtPRI- α* transcript levels was also observed
407 after treatment. The *PRI- α* gene is an SAR marker associated with salicylic acid (SA)
408 and SAR signaling. Our data showed that in Xanthi as well as in SR1 tobacco plants,
409 *PRI- α* transcript levels were highly induced, suggesting local defense and possible SAR
410 were induced by pGM. Importantly, pGM treatment did not induce any damage to the
411 fitness of the plants. In contrast, treated plants even showed slight growth enhancement
412 compared to water- and untreated plants (data not shown).

413 Recently, our group showed that treatment of tobacco roots and BY2 cells with *C.*
414 *herbarum* pGM induces oxidative stress and the expression of *PRI- α* and other defense-
415 related genes [23]. In addition, an HR-like response was observed when pGM was
416 infiltrated in tobacco leaves. To our knowledge, our results show for the first time that a
417 peptidogalactomannan isolated from the *C. herbarum* cell wall is able to induce local
418 and systemic defense responses in a whole plant. In the literature, other reports have
419 shown that distinct glycoproteins are able to confer SAR protection to a plant. Baillieul
420 *et al.* [33] and Cordelier *et al.* [34], using a 32 kDa glycoprotein named alpha-elicitin
421 secreted by the oomycete *Phytophthora megasperma*, demonstrated the induction of the
422 HR and the production of enzymes related to SAR after its administration in tobacco

423 leaf mesophyll. A reduction in the size of TMV-induced necrotic lesions in leaves was
424 observed after treatment with the glycoprotein. These studies, however, did not show a
425 reduction in the number of necrotic leaves, as observed in our work. In addition to the
426 reduction in the number of necrotic lesions observed on the HR TMV-resistant tobacco
427 Xanthi, we also observed a reduction in protection mediated by pGM in TMV-
428 susceptible SR1 cv., with a strong reduction in disease severity. Glucan 1,4-alpha-
429 glucosidase (BcGs1), isolated and purified from *Botrytis cinerea* culture supernatant,
430 was also able to induce SAR in tomato and tobacco plants [35]. Enzyme-treated plants
431 showed the induction of necrotic lesions that mimicked a typical HR. H₂O₂ production
432 was also increased in the treated tomato and tobacco plants that exhibited resistance to
433 *B. cinerea*, *Pseudomonas syringae* pv. tomato DC3000 and *Tobacco mosaic virus* along
434 with an increase in the transcript levels of the defense-related genes *PR1-α*, *TPK1b* and
435 prosystemin and a reduction of approximately 40% in TMV-induced necrotic lesions.
436 Several authors also reported the use of bacterial, fungal and oomycete culture filtrates
437 and/or secreted molecules to induce plant defense responses. The protein PemG1, an
438 elicitor molecule isolated from *Magnaporthe grisea* culture medium and expressed in an
439 *E. coli* heterologous system, induced resistance to bacterial pathogens in rice and
440 *Arabidopsis* [36]. Treatment with PemG1 did not inhibit bacterial growth but increased
441 plant resistance, indicating that PemG1 is an SAR elicitor. LI *et al.* [37] described a
442 novel HR-inducing protein elicitor, called PeFOC1, isolated from the culture filtrate of
443 *Fusarium oxysporum* f. sp. *cubense*. This protein induced ROS and an HR in tobacco
444 cells and induced the expression of *PR* genes (with upregulation of *PAL*, *EDS1*, *LOX*
445 and *PDF*). The SA and JA/ET signaling pathways were activated with the consequent
446 induction of callose and phenolic compound deposition, causing an immune response
447 and SAR in tobacco. A study by KWAK and collaborators [38] showed that an
448 uncharacterized fraction obtained from aqueous extraction of the fungus *Hericium*
449 *erinaceus* induces defense genes and promotes plant growth and death of the bacteria
450 that cause disease in tomatoes.
451 In our previous work, we observed that the expression of defense-related genes such as
452 *PrxNI*, *PAL*, *LOX* and the pathogen-related genes *PR1-α*, *PR-2* and *PR-3* were strongly
453 induced after the treatment of tobacco BY2 cells with pGM [23]. In the present work,
454 we observed that treatment of both tobacco Xanthi and SR1 with pGM also induced the
455 expression of *PR-1α*, *PR-2*, *PR-3*, *PR-5*, *LOX1*, *PAL* and *NtPrxNI*. The strong induction
456 of *PR1-α* and *PR-2* transcripts after pGM treatment suggests a possible SAR activation

457 by pGM. Despite small differences in the expression levels in Xanthi and SR1, we
458 observed that defense response induction mediated by pGM persisted for at least 3 and
459 5 days based on *PR1- α* and *PR-2* qRT-PCR results and the NBT assay.
460 Overexpression of *PR1- α* as well as other defense-related genes seems to directly
461 contribute to elicitor-mediated pathogen resistance, as already demonstrated by [39].
462 The ability of PR genes to enhance resistance against both biotic and abiotic stresses is
463 well documented. A strong induction of more than 2000x and 35x of the *PR1- α* gene
464 during the first 24 hours after pGM treatment was detected in both Xanthi and SR1
465 tobacco plants, respectively, showing that the expression of the *PR1- α* SAR marker is
466 induced in both tobacco plant cultivars. It is also interesting to highlight the increased
467 expression of transcripts from the hydrolytic β -1,3-endoglucanases (*PR-2*), commonly
468 activated in a fungal infection and another classical SAR marker, by treatment with
469 pGM. Activation of this gene is directly related to an antimicrobial effect due to
470 hydrolysis of β -1-3 glucans of the fungal wall, altering its integrity. Like β -1-3
471 endoglucanase, mRNAs of *PR-3* or chitinase, another well-known antifungal protein,
472 were strongly upregulated after 72 h of pGM treatment in both Xanthi and SR1 cv.
473 SINDELAROVA & SINDECOR [40] reported that both *PR-2a* and *PR-3* from
474 *Nicotiana tabacum* showed strong antiviral activity against TMV. In addition,
475 peroxidase and PAL transcripts, which were also strongly induced in our treated plants,
476 have also been shown to present antiviral activity [32, 41]. PAL may be induced by
477 ROS accumulation and is also considered an SAR component and a key enzyme in
478 defense, leading to the synthesis of antimicrobial molecules, including phytoalexins and
479 pathogen-related proteins and to the strengthening of the physical barrier against
480 pathogen colonization by deposition of structural polymers, such as lignin and callose,
481 at the infection site [42, 43]. The upregulation of *PR1- α* , *PR-2*, *PR-3*, *peroxidase* and
482 *PAL* genes observed after pGM treatment may explain the antiviral effects observed in
483 our TMV infection assays for both Xanthi and SR1 tobacco plants. Interestingly, Xanthi
484 and SR1 plants, however, showed differences in the time when these genes reached
485 their peak of induction. Apparently, the NN Xanthi cv. recognizes the fungal elicitor
486 faster than plants from SR1 cv.. Besides that, in Xanthi, the level of expression of these
487 genes were also higher than in SR1, with exception to *PR-3* and *PAL*. In combination,
488 these data suggest that Xanthi may be more prepared to respond against the pGM
489 PAMP/MAMP than SR1. However further experiments would be necessary to test this
490 hypothesis. As well, genome-wide transcriptome sequencing of pGM treated and

491 untreated samples would provide a better insight into the genes underlying pGM-
492 mediated defense response.

493

494 **Conclusions**

495 The results obtained in this work allow us to suggest that *C. herbarum* pGM is a
496 fungus PAMP able to induce the expression of *PRs* and *PAL*, *LOX* and *NtPrxNI* and to
497 activate other classical SAR markers, such as ROS induction and protection against
498 infection. Due to the importance of PR proteins in biotic and even abiotic stress
499 tolerance, several researchers are trying to obtain multi tolerant transgenic plants by
500 individual or dual PR overexpression (reviewed by [44]). Our data show that treatment
501 with pGM may induce at least four *PR* genes simultaneously that help plants resist
502 pathogen attack.

503

504 **Author contributions**

505 Conceptualization: CBM, MFSV and EB-B. Formal analysis: CBM, BBM, MFSV and
506 EB-B. Funding acquisition: MFSV and EB-B. Investigation: CBM. Methodology:
507 CBM, TFS. Project administration: MFSV and EB-B. Resources: MFSV and EB-B.
508 Supervision: MFSV and EB-B. Writing – original draft: CBM, MFSV and EB-B.
509 Writing – review & editing: CBM, TFS, EB-B and MFSV.

510 **Conflict of interest**

511 The authors declare that they have no conflict of interest.

512

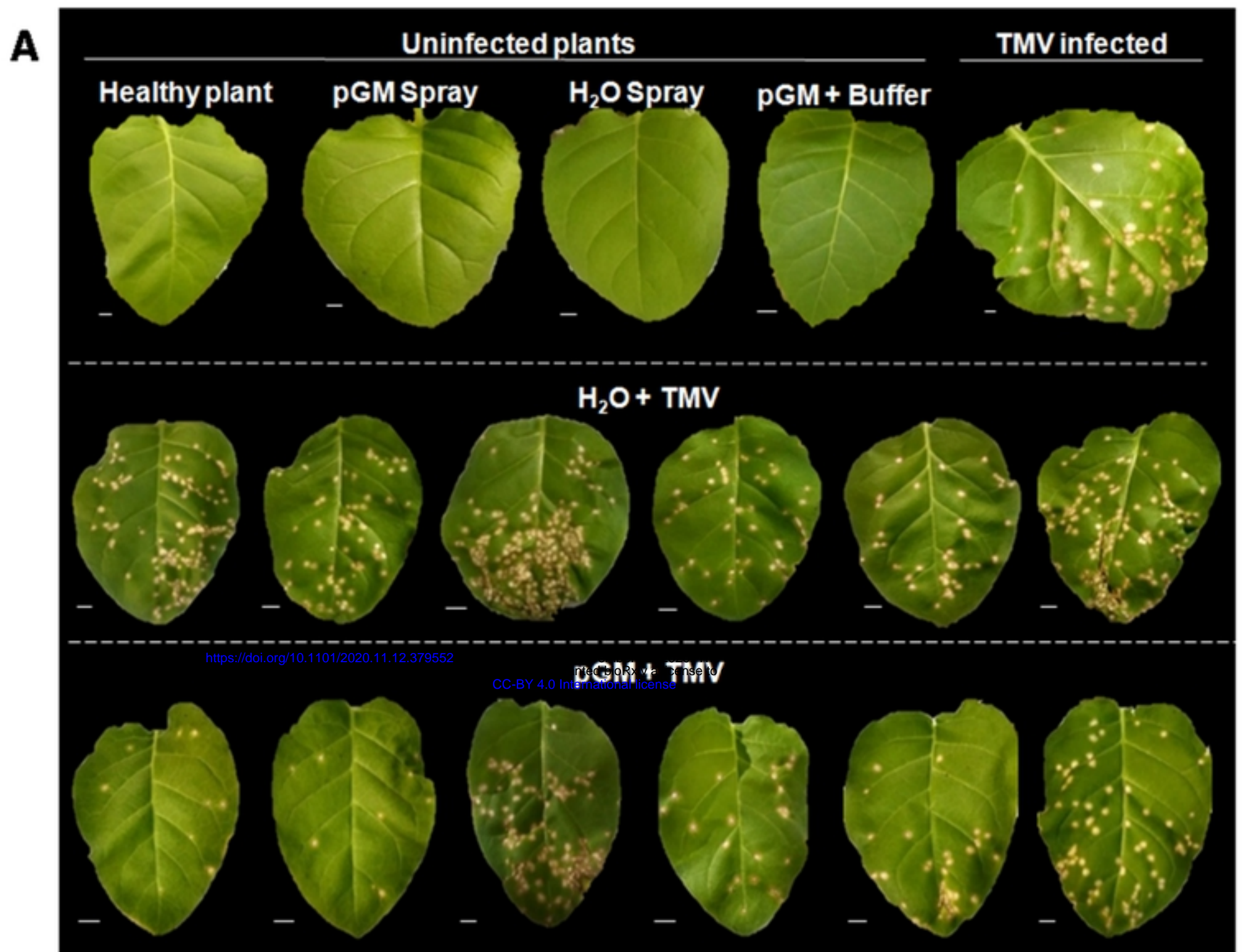
513 **References**

- 514 **1** JONES JD, DANGL JL. The plant immune system. *Nature* 2006;444: 323-329.
- 515 **2** TSUDA K, KATAGIRI F. Comparing signaling mechanisms engaged in pattern-
516 triggered and effector-triggered immunity. *Curr Opin Plant Biol.* 2010; 13: 459-465.
517 doi: 10.1016/j.pbi.2010.04.006
- 518 **3** LI B, HU F, ZHANG Q, ZHANG X, HONG Y. A cellular gene as a double
519 surveillance agent for plant to combat pathogen. *Plant Signal Behavior* 2013;8: 10

- 520 **4** FU ZQ, DONG X. Systemic acquired resistance: turning local infection into global
521 defense. *Annu Rev Plant Biol.* 2013;6: 839-863
- 522 **5** MUTHAMILARASAN M, PRASAD M. Plant innate immunity: an updated insight
523 into defense mechanisms. *J Biosci.* 2013;38(2): 433-449
- 524 **6** SHAH J, ZEIER J. Long-distance communication and signal amplification in systemic
525 acquired resistance. *Front Plant Sci.* 2013;4: 30
- 526 **7** KAMATHAM S, NEELA KB, PASUPULATI AK, PALLU R, SINGH SS,
527 GUDIPALLI P. Benzoylsalicylic acid isolated from seed coats of *Givotiarottleriformis*
528 induces systemic acquired resistance in tobacco and Arabidopsis. *Phytochemistry*
529 2016;126: 11-22 doi: 10.1016/j.phytochem.2016.03.002
- 530 **8** KLESSIG DF, CHOI HW, DEMPSEY DA. Systemic acquired resistance and salicylic
531 acid: past, present, and future. *MPMI* 2018;31(9): 871-888
- 532 **9** HEINZERLING L, FREW AJ, BINDSLEV-JENSEN C, BONINI S, BOUSQUET J,
533 RESCIANI M, CARLSEN KH, VAN CAUWENBERGE P, DARSOW U, FOKKENS,
534 WJ, HAAHTELA T, VAN HOECKE H, JESSBERGER B, KOWALSKI ML, KOPP,
535 T, LAHOZ CN, LODRUP CARLSEN KC, PAPADOPOULOS NG, RING J,
536 SCHMID-GRENDELMEIER P, VIGNOLA AM, WOHL S, ZUBERBIER T.
537 Standard skin prick testing and sensitization to inhalant allergens across Europe-a
538 survey from the GALEN network. *Allergy* 2005;60: 1287–1300
- 539 **10** FISCHER IH, REZENDE JAM. Diseases of passion flower (*Passifloras* pp.). Pest
540 technology, ed. Global Science Books 2008
- 541 **11** WISE K, ALLEN T, CHILVERS M, FASKE T, FREIJE A, ISAKEIT T, MUELLER D,
542 PRICE T, AGCENTER L, SISSON A, SMITH D, TENUTA A, WOLOSHUK C. Corn
543 disease management CPN2001. Crop Protection Network. [https://crop-protection-](https://crop-protection-network.s3.amazonaws.com/publications/cpn-2001-ear-rots.pdf)
544 [network.s3.amazonaws.com/publications/cpn-2001-ear-rots.pdf](https://crop-protection-network.s3.amazonaws.com/publications/cpn-2001-ear-rots.pdf) 2016
- 545 **12** SUSSEL AAB. Estudo da epidemiologia da verrugose-do-maracujazeiro. Embrapa
546 Cerrados, Ed. EMBRAPA, Brasília, DF. 2015
- 547 **13** VIANA FMP, FREIRE FCO, CARDOSO JE, VIDAL JC. Principais doenças do
548 maracujazeiro na região nordeste e seu controle. Comunicado Técnico on line 86, ISSN
549 1679-6535 Fortaleza, CE. 2003
- 550 **14** CABIB E, BOWERS B, SBURLATI A, SIVERMAN SJ. Fungal cell wall synthesis:
551 the construction of a biological structure. *Microbiol Sci* 1988; 5(12): 370-375
- 552 **15** FUKUDA EK, VASCONCELOS AFD, MATIAS AC, BARBOSA AM, DEKKER
553 RFH, SILVA MLC. Fungal cell wall polysaccharides: purification and characterization.
554 *Semina: Ciências Agrárias* 2009; 30(1): 117-134
- 555 **16** LATGÉ JP. Tasting the fungal cell wall. *Cell Microbiol* 2010;12(7): 863-872
- 556 **17** BARRETO-BERGTER E, FIGUEIREDO RT. Fungal glycans and the innate immune
557 recognition. *Front Cell Infect Microbiol* 2014;4: 145
- 558 **18** KLIS FM, BOORSMA A, DEGROOT PWJ. Cell wall construction in *Saccharomyces*
559 *cerevisiae*. *Yeast* 2006;23(3): 185–202
- 560 **19** LLOYD KO. Isolation, characterization and partial structure of peptidogalactomannan
561 from the yeast form of *Cladosporium werneckii*. *Biochem.* 1970;9: 3446-3453

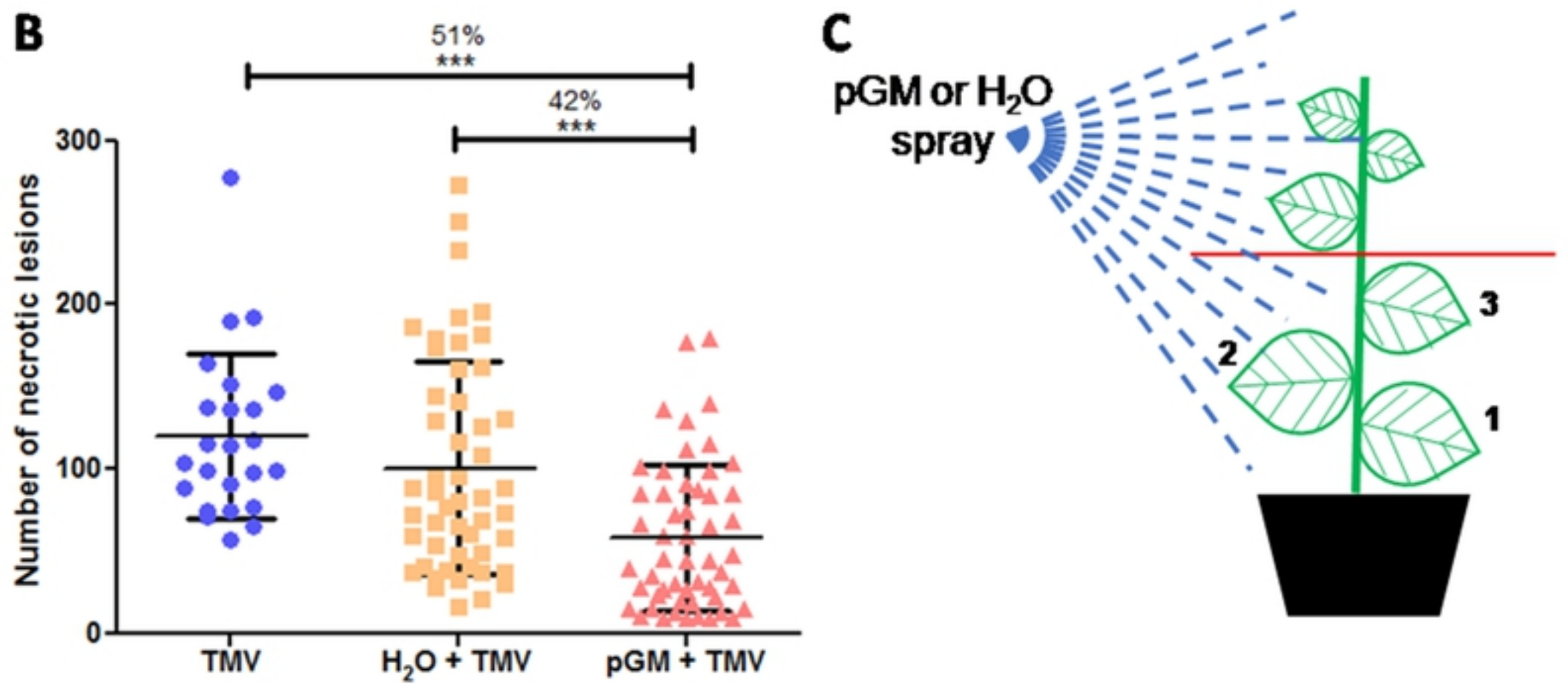
- 562 **20** LEITAO EA, BITTENCOURT VCB, HAIDO RMT, VALENTE AP, PETER-
563 KATALINIC J, LETZEL M, DE SOUZA LM, BARRETO-BERGTER E. β -
564 galactofuranose-containing *O*-linked oligosaccharides present in the cell wall
565 peptidogalactomannan of *Aspergillus fumigatus* contain immuno dominant epitopes.
566 *Glycobiology* 2003;13: 681-692
- 567 **21** SHIBATA N, SAITOH T, TADOKORO Y, OKAWA Y. The cell wall galactomannan
568 antigen from *Malassezia furfur* and *Malassezia pachydermatis* contains beta-1,6-linked
569 linear galactofuranosyl residues and its detection has diagnostic potential. *Microbiol.*
570 2009;155: 3420-3429
- 571 **22** CALIXTO ROR, MATTOS BB, BITTENCOURT V, LOPES L, SOUZA L,
572 SASSAKI, G, CIPRIANI T, SILVA M, BARRETO-BERGTER E. β -Galactofuranose
573 containing structures present in the cell wall of the saprophytic fungus *Cladosporium*
574 (*Hormoconis*) *resinae*. *Res Microbiol* 2010;161(8): 720-728
- 575 **23** MATTOS BB, MONTEBIANCO C, ROMANEL E, SILVA TF, BERNABÉ RB,
576 SIMAS-TOSIN F, SOUZA LM, SASSAKI GL, VASLIN MFS, BARRETO-
577 BERGTER E. A peptidogalactomannan isolated from *Cladosporium herbarum* induces
578 defense related genes in BY-2 tobacco cells. *Plant Physiol Biochem* 2018;126: 206-216
- 579 **24** FU Y, YIN H, WANG W, WANG M, ZHANG H, ZHAO X, DU Y. β -1,3-
580 Glucan with different degrees of polymerization induced different defense responses in
581 tobacco. *Carbohydr Polym.* 2011;86: 774-782
- 582 **25** DIJKSTRA J, JAGER CD. Practical Plant Virology. Protocols and Exercises.
583 Springer Lab Manuals, Springer. 1998
- 584 **26** OTSUKI Y, SHIMOMURA T, TAKEBE I. *Tobacco mosaic virus* multiplication and
585 expression of the N gene in necrotic responding tobacco varieties. *Virology* 1972; 50:
586 45-50
- 587 **27** MCKINNEY HH. Influence of soil temperature and moisture on infection of wheat
588 seedlings by *Helminthosporium sativum*. *J. Agric. Res.* 1923;26: 195–218
- 589 **28** BOURNONVILLE CFG, DÍAZ-RICCI JC. Quantitative determination of superoxide
590 in plant leaves using a modified NBT staining method. *Phytochem Anal.* 2011;22: 268–
591 271
- 592 **29** LIVAK KJ, SCHMITTGEN TD. Analysis of relative gene expression data using real-
593 time quantitative PCR and the $2^{-\Delta\Delta C_t}$ method. *Methods* 2001;25: 402-408
594 <https://doi.org/10.1006/meth.2001.1262>
- 595 **30** LIAO YW, SUN ZH, ZHOU YH, SHI K, LI X, ZHANG GQ, XIA XJ, CHEN ZX, YU
596 JQ. The role of hydrogen peroxide and nitric oxide in the induction of plant-encoded
597 RNA-dependent RNA polymerase 1 in the basal defense against *Tobacco mosaic*
598 *virus*. *PLoS One* 2013;8:e76090. <https://doi.org/10.1371/journal.pone.0076090>
- 599 **31** DENG XG, ZHU T, ZOU LJ, HAN XY, ZHOU X, XI DH, ZHANG DW, LIN HH.
600 Orchestration of hydrogen peroxide and nitric oxide in brassinosteroid-mediated
601 systemic virus resistance in *Nicotiana benthamiana*. *Plant J.* 2016;89: 478-493
602 <https://doi.org/10.1111/tpj.13120>

- 603 **32** HYODO K, SUZUKI N, MISE K, OKUNO T. Roles of superoxide anion and
604 hydrogen peroxide during replication of two unrelated plant RNA viruses in *Nicotiana*
605 *benthamiana*. Plant Signal Behavior 2017;12: 6
- 606 **33** BAILLIEUL F, GENETAT I, KOPP M, SAINDRENAN P, FRITIG B.
607 KAUFFERNANN S. A new elicitor of the hypersensitive response in tobacco: a fungal
608 glycoprotein elicits cell death, expression of defence genes, production of salicylic acid,
609 and induction of systemic acquired resistance. Plant J. 1995;8(4): 551-560
- 610 **34** CORDELIER S, de RUFFRAY P, FRITIGAND B, KAUFFMANN S. Biological and
611 molecular comparison between localized and systemic acquired resistance induced in
612 tobacco by a *Phytophthora megasperma* glycoprotein elicitor. Plant Mol Biol. 2003;51:
613 109–118
- 614 **35** ZHANG Y, ZHANG Y, QIU D, ZENG H, GUO L, YANG X. BcGs1, a glycoprotein
615 from *Botrytis cinerea*, elicits defence response and improves disease resistance in host
616 plants. Biochemical and Biophysical Res Commun. 2015; 457: 627-634
- 617 **36** PENG DH, QIU DW, RUAN LF, ZHOU CF, SUN M. Protein elicitor PemG1 from
618 *Magnaporthe grisea* induces systemic acquired resistance (SAR) in plants. MPMI
619 2011;24:(10): 1239-1246
- 620 **37** LI S, NIE H, QIU D, SHI M, YUAN Q (2019) A novel protein elicitor PeFOC1 from
621 *Fusarium oxysporum* triggers defense response and systemic resistance in tobacco.
622 Biochem Biophys Res Commun 514:1074-1080
- 623 **38** KWAK AM, MIN KJ, LEE SY, KANG HW. Water extract from spent mushroom
624 substrate of *Hericium erinaceus* suppresses bacterial wilt disease of tomato.
625 Microbiology 2015;43(3): 311-318
- 626 **39** LIU Y, LIU Q, TANG Y, DING W. NtPR1a regulates resistance to *Ralstonia*
627 *solanacearum* in *Nicotiana tabacum* via activating the defense-related genes. Biochem.
628 Biophys Res Commun. 2019;508: 940-945
- 629 **40** SINDELAROVA M, SINDELAR L. Isolation of pathogenesis-related proteins from
630 TMV-infected tobacco and their influence on infectivity of TMV. Plant Prot Sci. 2005;
631 41: 52-57
- 632 **41** MAKSIMOV IV, SOROKAN AV, BURKHANOVA GF, VESELOVA SV, YU AV,
633 SHEIN MY, AVALBAEV AM, DHAWARE PD, MEHETRE GT, SINGH BP,
634 KHAIRULLINR M. Mechanisms of plant tolerance to RNA viruses induced by plant-
635 growth-promoting microorganisms. Plants 2019;8:575. doi:10.3390/plants8120575
- 636 **42** ZHAO XM, SHE XP, YU W, LIANG XM, DU YG. Effects of oligochitosans on
637 tobacco cells and role of endogenous nitric oxide burst in the resistance of tobacco to
638 Tobacco mosaic virus. Plant Pathol J. 2007;89(1): 55-65
- 639 **43** NAZ R, BANO A, WILSON NL, GUEST D, ROBERTS TH. Pathogenesis-related
640 protein expression in the apoplast of wheat leaves protected against leaf rust following
641 application of plant extracts. Phytopathology 2014;104: 933-944
- 642 **44** ALI S, GANAI BA, KAMILI AN, BHAT AA, MIR ZA, BHAT, JA, TYAGI A, ISLAM
643 ST, MUSHTAQ M, YADAV P, RAWAT S, GROVER A (2018) Pathogenesis-related
644 proteins and peptides as promising tools for engineering plants with multiple stress
645 tolerance. Microbiol Res 212-213:29-37



<https://doi.org/10.1101/2020.11.12.379552>

bioRxiv preprint doi: <https://doi.org/10.1101/2020.11.12.379552>; this version posted November 12, 2020. The copyright holder for this preprint (which was not certified by peer review) is the author/funder, who has granted bioRxiv a license to display the preprint in perpetuity. It is made available under aCC-BY 4.0 International license.



D

Leave position	TMV	H ₂ O + TMV	pGM + TMV
1	104,88 ± 71,16a	52,61 ± 25,01b	55,11 ± 42,89b
2	136,75 ± 40,99a	133,59 ± 62,90a	72,61 ± 45,89b
3	118,50 ± 31,16a	121,53 ± 69,23a	46,76 ± 43,56b
Number of plants	10	20	20

Figure 1

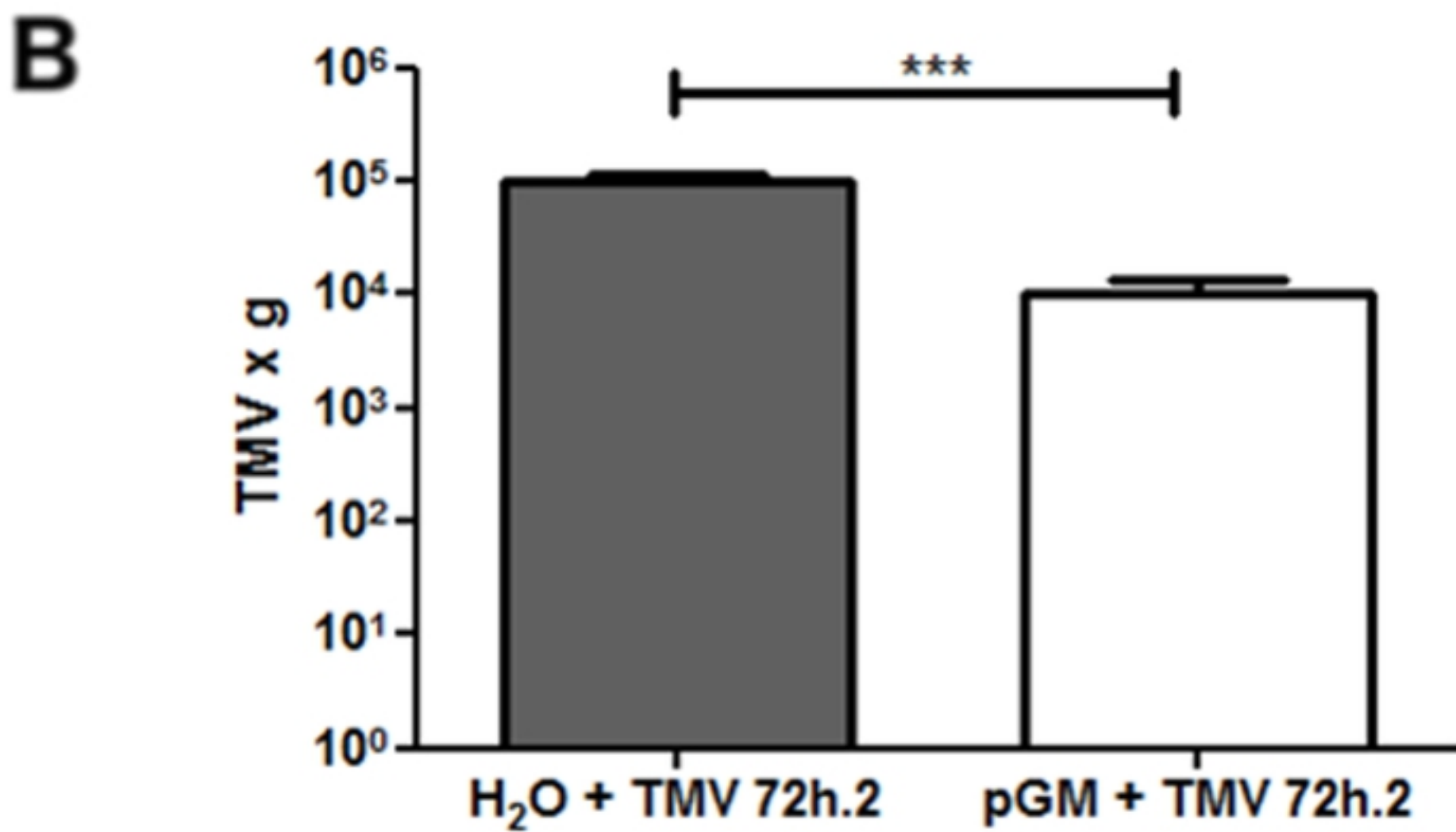
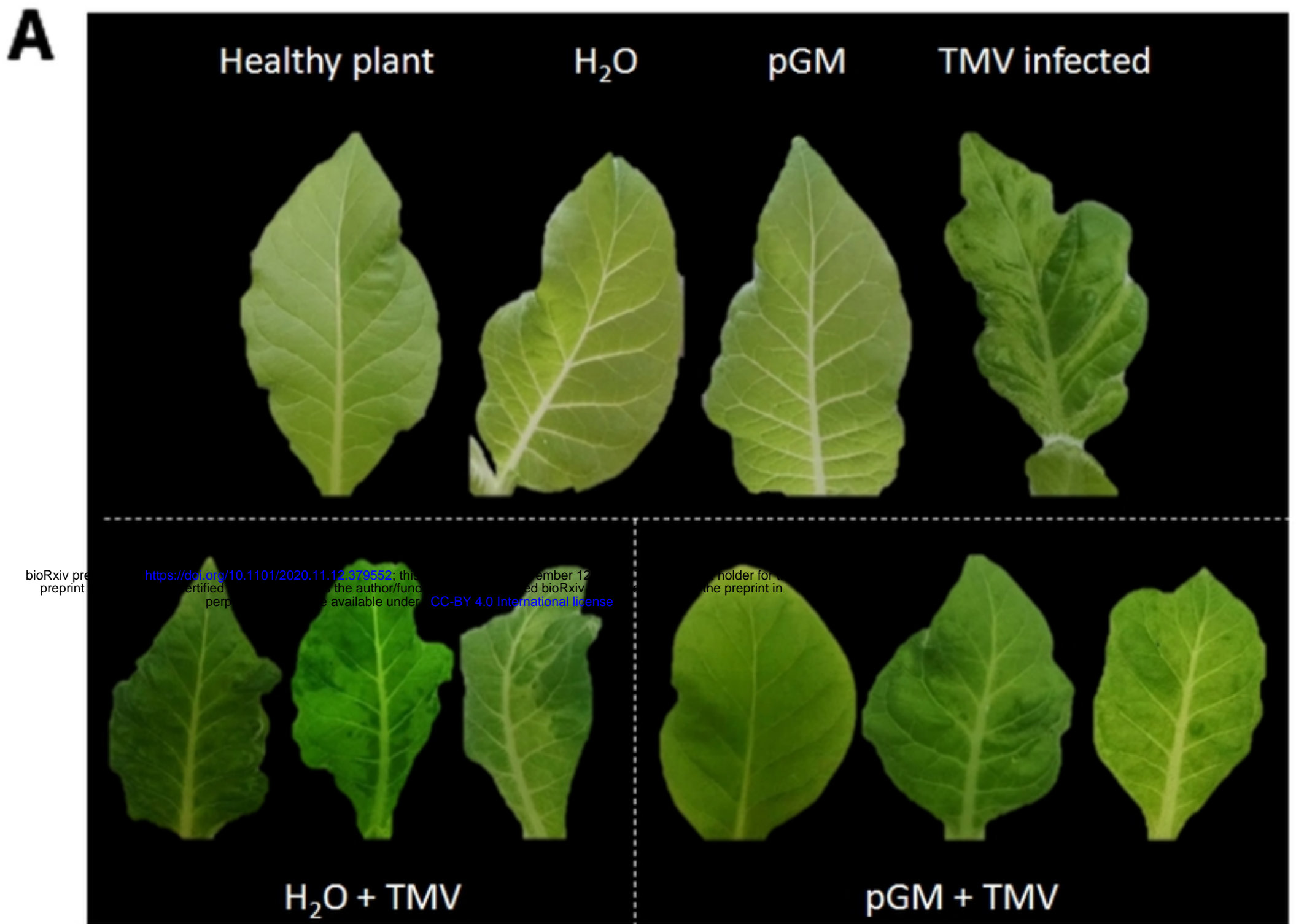


Figure 2

Healthy plant 100 $\mu\text{g.ml}^{-1}$ 200 $\mu\text{g.ml}^{-1}$ 400 $\mu\text{g.ml}^{-1}$ 600 $\mu\text{g.ml}^{-1}$

1 dap

bioRxiv preprint doi: <https://doi.org/10.1101/2020.11.12.379552>; this version posted November 12, 2020. The copyright holder for this preprint (which was not certified by peer review) is the author/funder, who has granted bioRxiv a license to display the preprint in perpetuity. It is made available under aCC-BY 4.0 International license.

3 dap

8dap

10dap

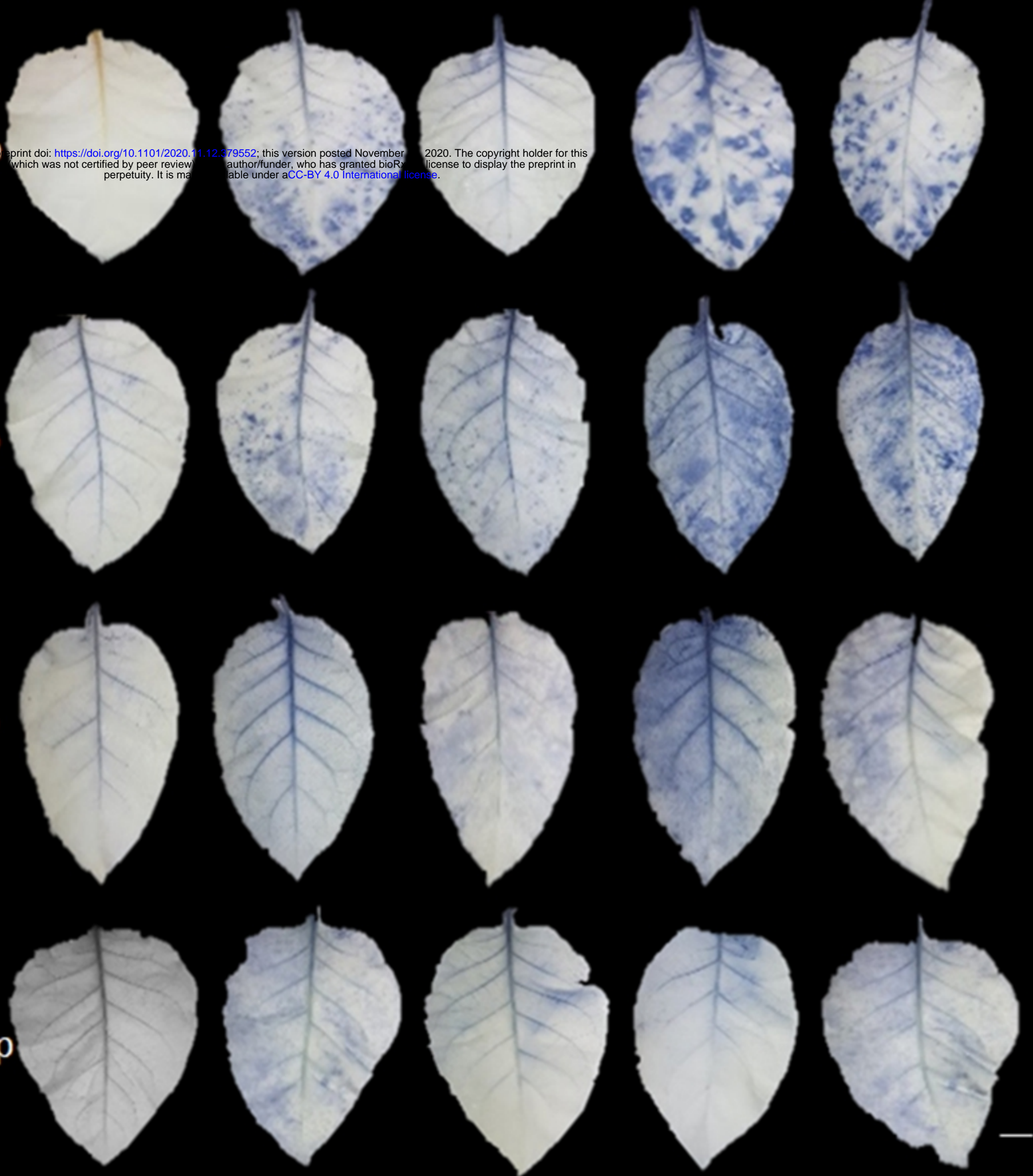


Figure 3

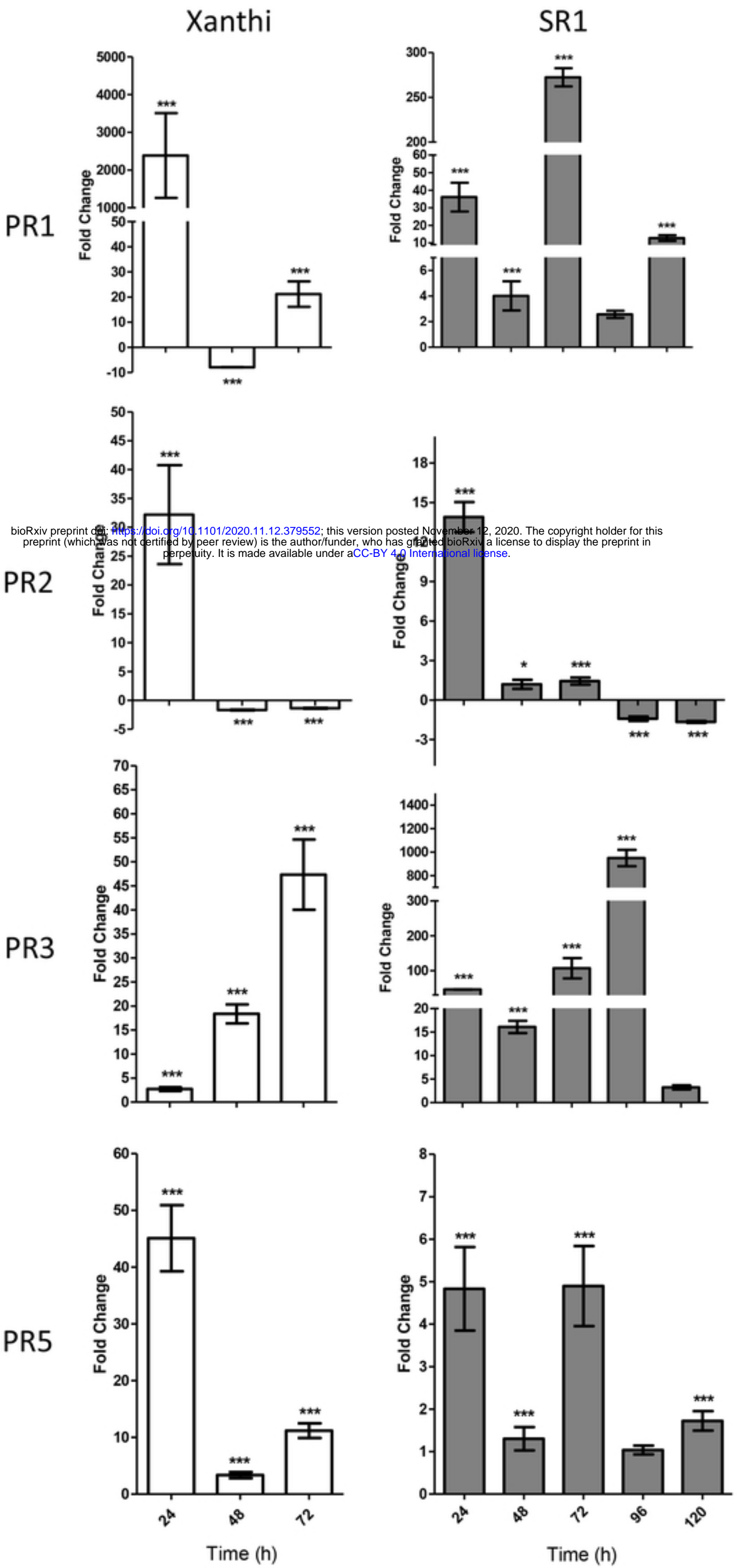


Figure 4

bioRxiv preprint doi: <https://doi.org/10.1101/2020.11.12.379552>; this version posted November 12, 2020. The copyright holder for this preprint (which was not certified by peer review) is the author/funder, who has granted bioRxiv a license to display the preprint in perpetuity. It is made available under aCC-BY 4.0 International license.

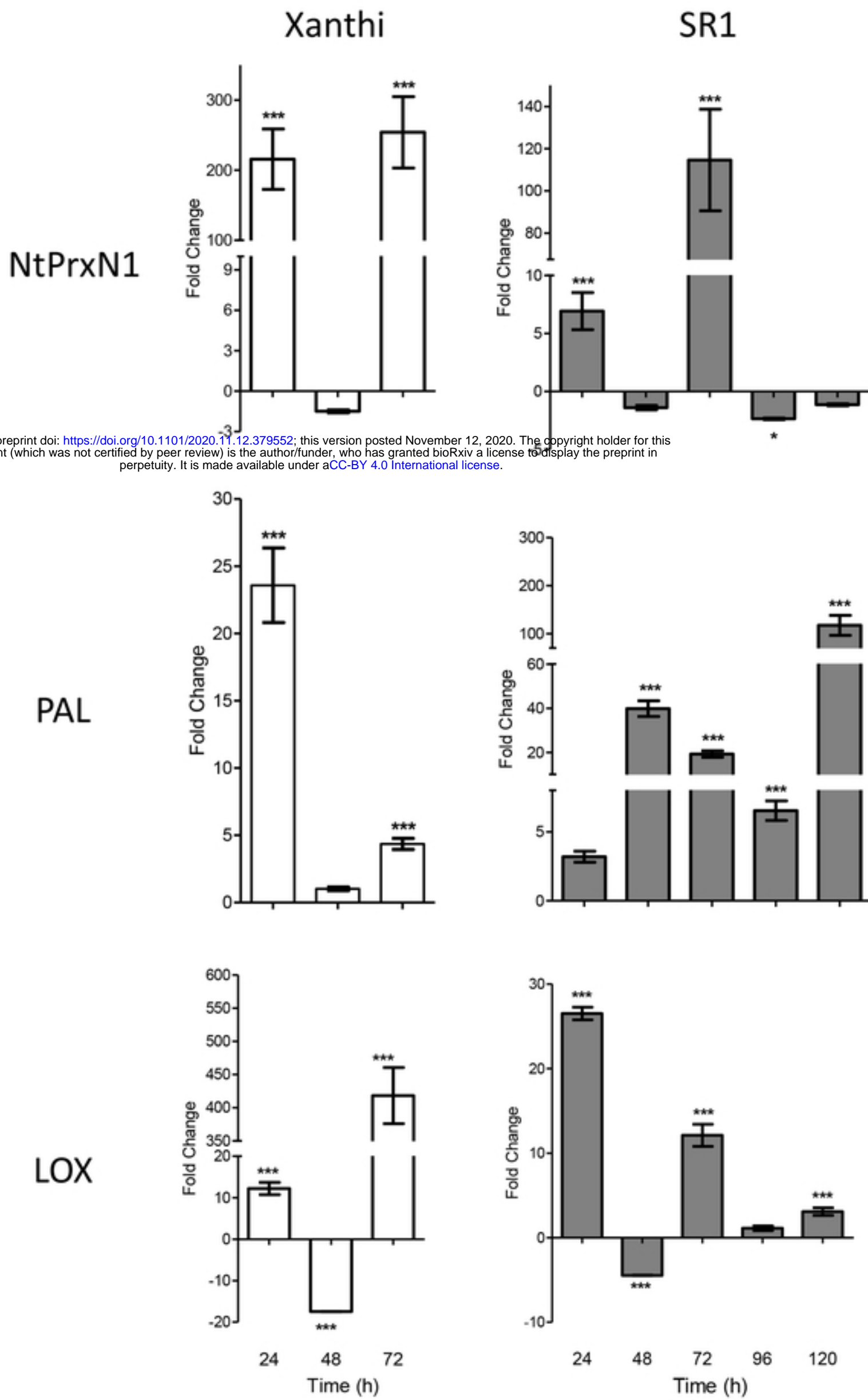


Figure 5